



Nuclear magnetic relaxation of methyl protons in a paramagnetic protein: cross-correlation effects

Pravat K. Mandal, P.K. Madhu, Norbert Müller*

Institut für Chemie, Organische Chemie, Johannes Kepler Universität, Altenbergerstrasse 69, Linz A 4040, Austria

Received 13 January 2000; in final form 21 February 2000

Abstract

Multi-exponential relaxation and concomitant relaxation allowed multiple quantum coherence among methyl protons in paramagnetic proteins arising from cross-correlation between Curie spin relaxation (CSR) and dipolar relaxation (DD) are investigated. Numerical simulations and semi-quantitative multi-quantum experiments in the cyanide-inhibited paramagnetic protein horseradish peroxidase underscore the presence of $CSR \times DD$ cross-terms. The magnitude of the resulting two-spin order depends on the distance and relative orientation of the methyl axis to the paramagnetic centre which can be exploited to derive structural constraints. © 2000 Elsevier Science B.V. All rights reserved.

1. Introduction

The simultaneous presence of various spin interactions of the same orbital tensorial ranks can give rise to interference or cross-correlation effects and have been the subject of a plethora of theoretical and experimental investigations since the early days of nuclear magnetic resonance (NMR) spectroscopy [1]. Multi-exponential longitudinal and transverse relaxation behaviour that ultimately lead to so-called relaxation allowed coherence transfer (RACT), earlier referred to as ‘forbidden cross-peaks’ in multi-dimensional spectra [2,3], as well as multiplet effects [4,5], differential line broadening [6], dynamic frequency shifts [7] are characteristic of cross-correlation phenomena. Apart from the fundamental interest in these physical phenomena, geometrical and dy-

namical information are contained in relaxation data [8–10]. The ability for experimental observation and exploitation of cross-correlation effects has increased with the availability of higher magnetic fields, where interference effects become pronounced, and with the investigation of molecules tailored to enhance such effects [11,12].

A characteristic signature of the cross-correlation phenomenon is the generation of multi-spin orders, for instance, two- and three-spin order in a methyl group. $CSA \times DD$ type of cross-correlation creates two-spin order while $DD \times DD$ cross-correlation results in three-spin order [7]. The presence of these multi-spin orders leads to multiplet effects that have been observed in various systems. The amplitudes of these spin order terms reflect signatures of the types and measures of the strengths of cross-correlation processes.

Most studies on cross-correlation between the relaxation mechanisms have been focussed on diamagnetic molecules including proteins. Recently the

* Corresponding author. Fax: +43-732-2468-747; e-mail: norbert.mueller@jk.uni-linz.ac.at

presence of cross-correlation phenomena has also been reported in paramagnetic systems which feature a unique relaxation mechanism, namely, the Curie spin relaxation (CSR), involving unpaired electron spins [13–19]. Although the pronounced effects of a paramagnetic centre on enhancing nuclear relaxation have been well documented and called the ‘contact term’ [20,21] arising from the presence of the electron, the importance of CSR due to a paramagnetic centre, the so-called ‘susceptibility’ contribution, has been recognized only later [22,23]. While the contact term corresponds to relaxation of the nuclei by the electron magnetic field which is modulated only by the molecular motion, the susceptibility term is due to relaxation by fluctuating part of the electronic field modulated both by electronic spin relaxation and molecular motion or in other words relaxation by the dipolar field of the thermally averaged electronic spin [22]. Studies on the cross-correlation between CSR and internuclear dipolar interaction (DD) showed that this interference can generate cross-peaks in COSY spectra even in the absence of homonuclear scalar couplings [13]. Cross-correlations involving internuclear and nucleus–electron interactions of non-degenerate nuclear spins have recently been successfully used to derive angular constraints [19]. Cross-correlation effects involving the isochronous methyl protons carry the potential of increasing the number of experimental structural constraints for methyl bearing residues in paramagnetic proteins, which are abundant in the hydrophobic cores of proteins thereby paving the way for a better refinement of their structures.

In this Letter, we report the influence of a localized paramagnetic centre on the relaxation behaviour of methyl protons using cyanide-ligated horseradish peroxidase (HRP-CN) as a model paramagnetic protein which has an embedded Fe^{3+} heme site of electron spin $S_e = 1/2$. The purpose of this investigation is to examine the process of generating multi-quantum coherences involving only the methyl protons due to the cross-terms involving CSR and its subsequent conversion to observable single quantum coherences with a nearby proton spin. The fundamental differences of the relaxation behaviour of methyl protons in diamagnetic proteins are highlighted by comparison to hen egg white (HEW) lysozyme.

2. Experimental

3 mM HRP (Boehringer-Mannheim) in 99.99% D_2O and HEW lysozyme (Sigma) of molecular weights 42.5 and 14.8 kD were used for the NMR experiments. The low spin ($S_e = 1/2$) cyanide complex of HRP (HRP-CN) was prepared by adding excess KCN to the protein solution. The pH of the solutions was adjusted to 6.77 (HRP-CN) and 4.56 (lysozyme) by adding NaOD and/or DCl. Sample volumes were 0.5 cm^3 (5 mm tubes). All NMR

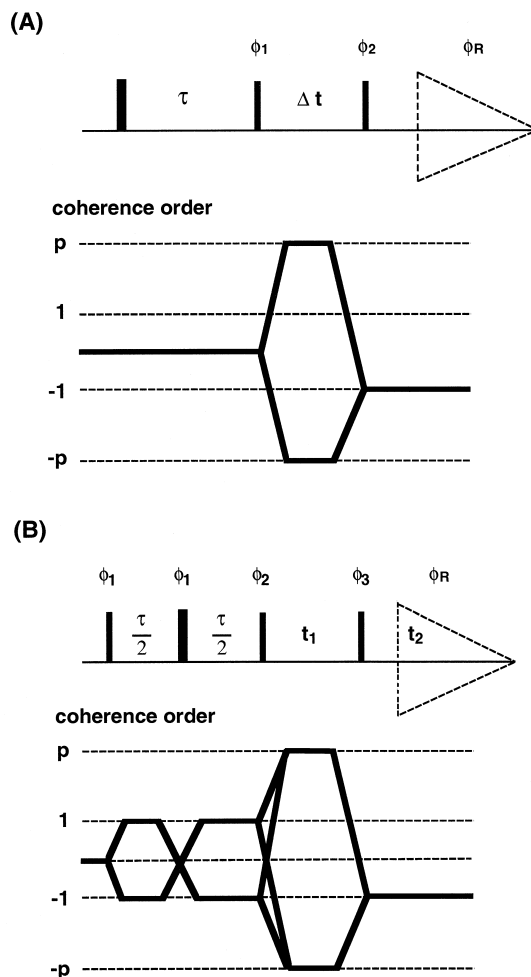


Fig. 1. Pulse sequences used for (A) MERCY and (B) multi-quantum correlation experiments. In (A) and (B) appropriate phase cycling with $\phi_2 = \phi_1 + \frac{\pi}{2}$ was employed for selecting 2Q and 3Q coherences. A spoiler gradient of strength 30 G/cm was used in the MERCY experiment during the τ period.

experiments were performed on a Bruker Avance DRX-500 MHz spectrometer equipped with a triple-gradient triple-resonance inverse detection probe at 40° (HRP) or 30° (lysozyme). The following experiments were performed on both the samples: one-dimensional version of 2Q and 3Q multi-exponential relaxation spectroscopy (MERCY) [24] and two-dimensional 2Q and 3Q spectroscopy. Fig. 1 shows the pulse sequences used for the experiments, the parameters of which are indicated in the figure captions of the respective spectra. Solvent signal presaturation was employed for suppression of residual water signals in all the experiments.

3. Theory

The irreducible spin tensors for the DD ($V_{DD}^{(i)}$), CSA ($V_{CSA}^{(i)}$) [25,26] and CSR ($V_{CSR}^{(i)}$) [17] ($i = 0, \pm 1, \pm 2$) may be written in terms of Cartesian (I_z) and shift operators (I_+ and I_-) as

$$V_{DD}^{(0)} = -\frac{1}{12}(4I_z^2 - I_+I_- - I_-I_+),$$

$$V_{DD}^{(\pm 1)} = \pm \frac{1}{2\sqrt{6}}(I_zI_{\pm} + I_{\pm}I_z),$$

$$V_{DD}^{(\pm 2)} = -\frac{1}{2\sqrt{6}}I_{\pm}^2,$$

$$V_{CSR}^{(0)} = V_{CSA}^{(0)} = \sqrt{\frac{8}{15}}I_z,$$

$$V_{CSR}^{(\pm 1)} = V_{CSA}^{(\pm 1)} = \mp \frac{1}{\sqrt{5}}I_{\pm},$$

$$V_{CSR}^{(\pm 2)} = V_{CSA}^{(\pm 2)} = 0. \quad (1)$$

In the above, the constant coefficients have been adjusted such that the spin part of both CSA and CSR are equal and any differences are moved to the spatial part for convenience. It may be appreciated that in the irreducible representation the form of CSR is analogous to that of CSA although the former is a dipolar coupling interaction between the electron and the proton spin and the latter is a single spin interaction with an external magnetic field. This analogy holds good as long as the electron Hamiltonian is not manipulated. Since the form of the CSA and CSR Hamiltonians is identical the characteristic

signatures of cross-correlations involving CSR or CSA is the creation of two-spin order. This aspect is the focal point in the following.

The spectral densities associated with the various interactions are given as

$$J_k(\omega) = \rho_k \frac{\tau_c}{1 + (\omega\tau_c)^2} \quad (2)$$

where k stands for either DD, CSA or CSR, ω is the Larmor frequency of the protons and τ_c the correlation time. The constant coefficients ρ_k s can be expressed as [13,26]

$$\rho_{DD} = \frac{9}{20} \left(\frac{\mu_0}{4\pi} \right)^2 \gamma_H^4 \hbar^2 r_{HH}^{-6}$$

$$\rho_{CSA} = \frac{1}{5} \gamma_H^2 B_0^2 \Delta \sigma_H^2 \quad (3)$$

$$\rho_{CSR} = \frac{9}{4} \left(\frac{\mu_0}{4\pi} \right)^2 \gamma_H^2 r_{He}^{-6} \hbar^2 \left[\frac{g_e \beta_m \gamma_e B_0 S_e (S_e + 1)}{3kT} \right]^2.$$

In the above, the various symbols have the following significance: B_0 the magnetic field, γ_H and γ_e the gyromagnetic ratios of the proton and electron respectively, r_{HH} the distance between the methyl protons, r_{He} the distance between the electron and the centre of the gravity of the methyl protons, \hbar the Planck's constant divided by 2π , $\Delta \sigma_H$ the chemical shift anisotropy of the methyl protons, g_e the electronic g factor of value 2, S_e the electron spin quantum number, β_m the Bohr magneton, k the Boltzmann constant and T the temperature. The influence of self-relaxation of the electron, the so-called contact term, is added explicitly to the diagonal elements of the Redfield matrix with the form of the spectral densities for longitudinal (J_e^{long}) and transverse (J_e^{trans}) relaxation due to the paramagnetic centre given respectively by Refs. [23,27]

$$J_e^{\text{long}}(\omega) = \frac{6}{15} \left(\frac{\mu_0}{4\pi} \right)^2 (g_e \beta_m \gamma_H r_{He}^{-6})^2$$

$$\times \left[\frac{S_e(S_e + 1)}{3} \right] \frac{T_{1e}}{1 + (\omega T_{1e})^2}$$

$$J_e^{\text{trans}}(\omega) = \frac{1}{15} \left(\frac{\mu_0}{4\pi} \right)^2 (g_e \beta_m \gamma_H r_{He}^{-6})^2$$

$$\times \left[\frac{S_e(S_e + 1)}{3} \right] \left[4T_{1e} + \frac{3T_{1e}}{1 + (\omega T_{1e})^2} \right] \quad (4)$$

where T_{1e} is the electron spin–lattice relaxation time. The approximations implicit in arriving at the above expressions and the explicit expressions for the Redfield matrix elements will be discussed in detail elsewhere. The spectral density associated with the cross-correlation terms is generally written as

$$J_{kl}(\omega) = P_2 \cos(\theta) \sqrt{J_k(\omega) J_l(\omega)} \quad (5)$$

where $P_2 \cos(\theta)$ is the Legendre polynomial of order 2 and k and l correspond to any of the relaxation interactions under consideration here. In the case of CSR \times DD cross-correlation the angle θ is the angle subtended by the \mathbf{r}_{He} with the normal to the methyl protons plane, coinciding with the methyl C_3 rotation axis, as indicated in Fig. 2.

As in the earlier approaches we treat the energy levels of the three methyl protons in the symmetry adapted base approach as a superposition of a spin 3/2 and two-spin 1/2 group spins [3]. Since multiple quantum coherence is only possible within the $F = 3/2$ group, the discussion will be restricted to this subspace. We use transfer functions, $f_{l' l}^{(p)}$, to describe the multiexponential relaxation of degenerate spins in a reducible spherical tensor base [26]. These transfer functions describe the time evolution

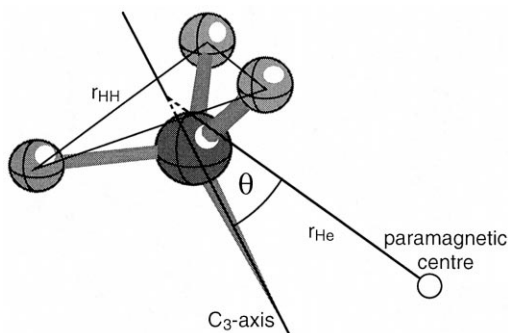


Fig. 2. The geometry of the system of a methyl group and a paramagnetic centre considered for the simulations shown in Fig. 3. A uniform distance of 1.46 Å is assumed between the protons in the methyl group, and 7 Å between the electron and the centre of the gravity of methyl protons. The angle, θ , which such a vector makes with the C_3 axis of methyl group rotation has been assumed to be zero in the simulations to maximize the effect of cross-correlations.

and partial interconversion of population and coherence as

$$T_{l' p} \sum_{l' \geq |p|} f_{l' l}^{(p)}(t) T_{l' p} \quad (6)$$

and are given by

$$f_{l' l}^{(p)}(t) = \sum_n a_{n l' l} e^{R_n t} \quad (7)$$

In the above \hat{R} is the relaxation superoperator, $T_{l' p}$ represent single- and multi-spin orders with l denoting the rank of the tensor operator and p the coherence level. The coefficients $a_{n l' l}$ and the rates R_n are obtained as the eigenvectors and eigenvalues of the matrix representation of \hat{R} which are calculated from Redfield's theory [28].

Depending upon which cross-correlation terms are active during the relaxation delay, one can expect relaxation induced 2Q or 3Q signals in multi-quantum experiments. 3QC can arise only from rank 3 term, $T_{3,0}$, the presence of which in the $F = 3/2$ subspace is caused by the DD \times DD cross-correlation terms. 2QC can arise from both rank 2 and 3 terms, $T_{2,0}$ and $T_{3,0}$, the former originating via CSA \times DD or CSR \times DD cross-correlated relaxation and the latter via DD \times DD cross-correlation terms. The relative strengths of the different cross-correlated interactions determine the amplitude of the peaks on the MQ-diagonal ($\omega_1 = p\omega_2$) in either the 2Q or 3Q experiments.

Since the unwanted transformation $T_{3,0} \rightarrow T_{3,\pm 2}$ has a flip angle dependence of $\sqrt{(15/8)} \sin^2 \beta \cos \beta$ [3,29] while $T_{2,0} \rightarrow T_{2,\pm 2}$ has a dependence of $\sqrt{(3/8)} \sin^2 \beta$ [3,29] which are the Wigner coefficients, the undesired pathway is suppressed when using a 90° pulse [3]. This ensures that in the MERCY experiment the peaks come from rank 2 tensors characteristic of cross-correlations involving CSR \times DD and CSA \times DD.

As in the 2Q MERCY experiment in the 2Q correlation experiment the 2Q diagonal peaks ($\omega_1 = p\omega_2$) arise only from rank 2 terms due to the flip angle dependence [3,29]. While a 3Q methyl signal implies the presence of a rank 3 term, $T_{3,\pm 1}$, at the end of τ (Fig. 1b), the 2Q counterpart shows a rank 2 term, $T_{2,\pm 1}$.

To characterize the effect of the cross-correlated interactions considered here, the transfer functions, $f_{11}^{(\pm 1)}, f_{21}^{(\pm 1)}$ and $f_{31}^{(\pm 1)}$ and $f_{11}^{(0)}, f_{21}^{(0)}$ and $f_{31}^{(0)}$ involved in the conversion processes

$$T_{1,\pm 1} \rightarrow f_{11}^{(\pm 1)}T_{1,\pm 1} + f_{21}^{(\pm 1)}T_{2,\pm 1} + f_{31}^{(\pm 1)}T_{3,\pm 1} \quad (8)$$

$$T_{1,0} \rightarrow f_{11}^{(0)}T_{1,0} + f_{21}^{(0)}T_{2,0} + f_{31}^{(0)}T_{3,0} \quad (9)$$

have been calculated numerically. Eq. (8) deals with the creation of rank 2 and 3 one-quantum coherences (1QC) from transverse magnetization of rank 1. Eq. (9) characterizes the behaviour of longitudinal magnetization in the inversion recovery type MERCY [24] experiments. Fig. 3 shows plots of each of these for a typical correlation time of 5×10^{-9} s comparing the case of DD \times DD and CSA \times DD cross-correlation only, Fig. 3A,B, to the case of presence of additional CSR \times DD cross-correlation terms, Fig.

3C,D. The following features are especially noteworthy: (i) The tendency of cross-terms involving CSR to dominate the relaxation processes is evident from the evolution behaviour of $f_{21}^{(\pm 1)}$ and $f_{21}^{(0)}$ (ii) The electron spin clearly affects $f_{11}^{(\pm 1)}$ and $f_{11}^{(0)}$ in that the transverse and longitudinal relaxation rates are both accelerated, although the influence of the electron spin on transverse relaxation is small compared to its influence on longitudinal relaxation (iii) The transfer functions $f_{21}^{(\pm 1)}$ and $f_{31}^{(\pm 1)}$ become comparable, at the time $f_{21}^{(\pm 1)}$ has a maximum amplitude, under the influence of cross-correlated paramagnetic relaxation. The maximum of $f_{21}^{(\pm 1)}$ for the case of CSR \times DD cross-correlation occurs after ca. 7 ms of 1Q evolution. In contrast $f_{21}^{(\pm 1)}$, caused by CSA \times DD cross-correlation, remains small in the absence of electron paramagnetism.

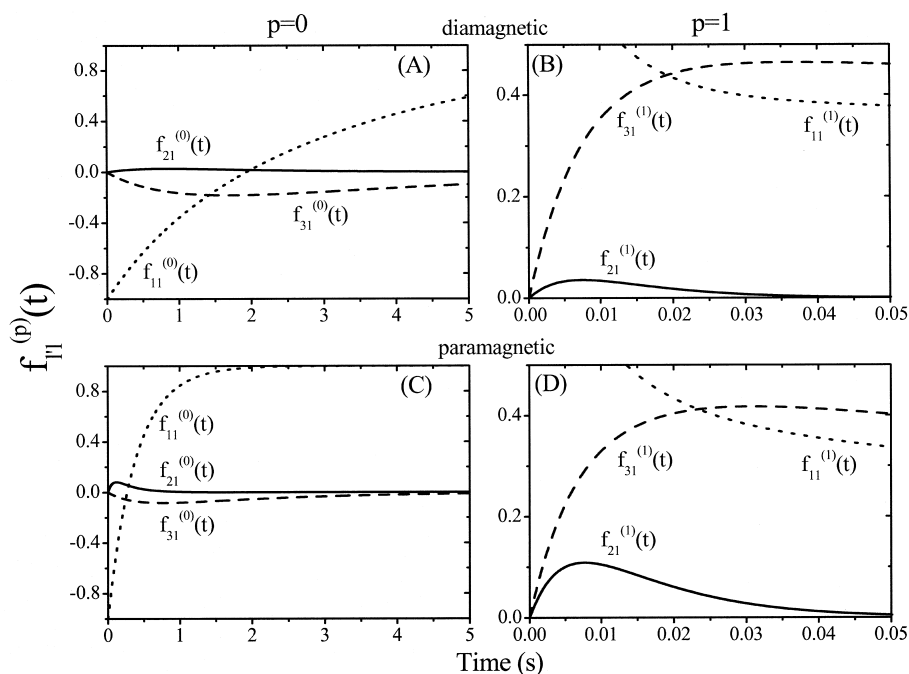


Fig. 3. The time dependence of the transfer functions, $f_{ll}^{(\pm p)}(t)$, pertaining to the longitudinal magnetization, $p = 0$, (A) and (C) and single quantum coherence, $p = \pm 1$, (B) and (D) assuming 500 MHz for the proton resonance frequency for a correlation time of 5 ns. The top trace corresponds to the situation prevailing in a diamagnetic system where a methyl proton CSA of $\Delta\sigma = 10$ ppm is assumed [34]. The bottom trace corresponds to a scenario in a paramagnetic system where the CSR mechanism is taken into account additionally. The geometry as described in Fig. 2 and an electron spin–lattice relaxation time, T_{1e} , of 10^{-12} s according to the literature [33] are considered for this simulation. The continuous lines represent $f_{21}^{(\pm p)}(t)$, dashed lines, $f_{31}^{(\pm p)}(t)$ and dotted lines, $f_{11}^{(\pm p)}(t)$. Note that it is $-f_{31}^{(\pm 1)}(t)$ which is always positive that has been plotted in (B) and (D).

4. Results and discussions

In HRP-CN a Fe^{3+} ion with $S_e = 1/2$ is embedded in a porphyrin ring. The ring bears four methyl groups which are 6 Å away from the Fe^{3+} site, designated as 1- CH_3 , 3- CH_3 , 5- CH_3 and 8- CH_3 [30]. The influence of the paramagnetic relaxation on these methyl groups is high as a consequence of their proximity to the paramagnetic centre, which impedes detailed observation of these methyl signals due to their large line widths of the order of 300 Hz [13]. Concomitantly, the maximum amplitude of the transfer functions occur at very short times that are experimentally difficult to access. From the three-dimensional crystallographic structure of this protein it is known that the Ile-244 residue is close to the 8- CH_3 [31]. The γCH_3 of this isoleucine residue is about 8 Å away from the Fe^{3+} centre. To confirm the assignment of I-244 γCH_3 , a steady state NOE experiment was performed, Fig. 4E. The well resolved signal of I-244 γCH_3 at 0.99 ppm [32] is monitored in the following experiments. For comparison, identical experiments were carried out on both the paramagnetic and diamagnetic proteins. One set of experiments was designed to select two-spin order (via 2QC) which is the characteristic signature of both $\text{CSR} \times \text{DD}$ and $\text{CSA} \times \text{DD}$ cross-correlation. The second set of experiments selected three-spin order (via 3QC) which is the signature of $\text{DD} \times \text{DD}$ cross-correlation.

Fig. 4 shows spectra obtained by one-dimensional versions of the 2Q and 3Q MERCY experiment (Fig. 1A) on both the proteins. It can be clearly seen that while a significant amount of 2Q signal is generated in the sample of paramagnetic protein, 3Q signal dominates in the diamagnetic protein. This indicates that a large amount of two-spin order is generated in the paramagnetic protein while a three-spin order prevails in the diamagnetic protein. This brings out what might be called fingerprints of $\text{CSR} \times \text{DD}$ cross-correlation in the paramagnetic protein and of $\text{DD} \times \text{DD}$ cross-correlation in the diamagnetic protein. It should be noted that a MERCY experiment typically convolutes longitudinal (in the τ period) and transverse relaxation effects (in the detection period). Under the conditions used here the susceptibility term due to the paramagnetic centre has a bigger influence on transverse relaxation than on

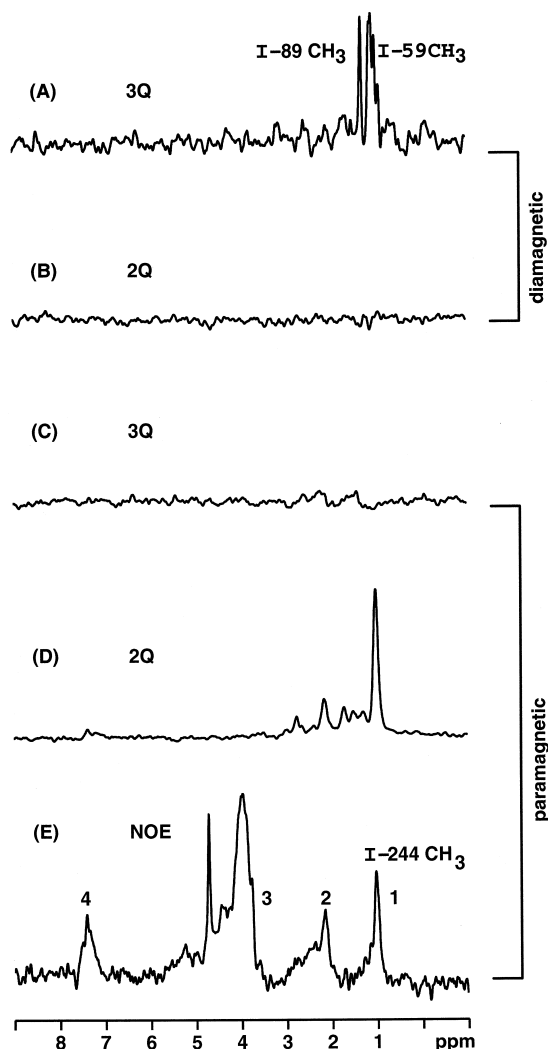
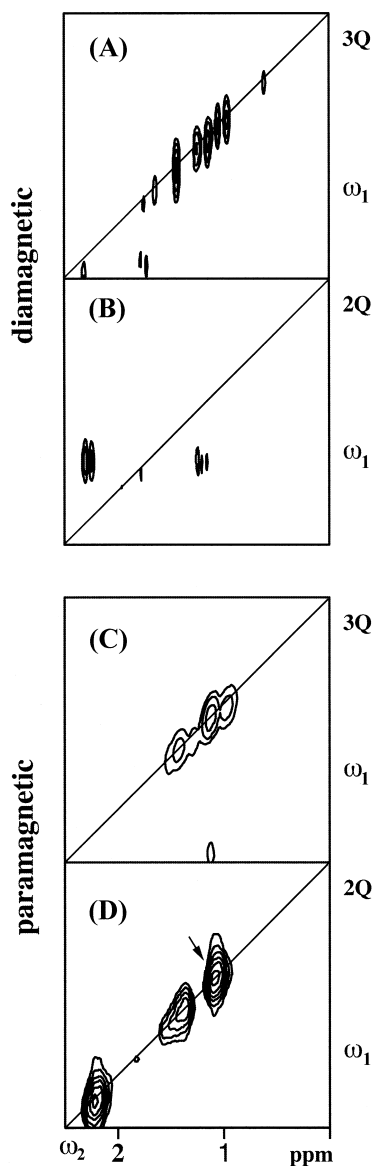


Fig. 4. The spectra resulting from one-dimensional 2Q and 3Q versions of MERCY on lysozyme (A,B), and on HRP (C,D). (E) shows the result of a steady state NOE experiment performed to identify the I-244 γCH_3 resonance. For the experiments on HRP, 12K transients were accumulated with a recycle delay of 1 s. The relaxation delay, τ , for HRP was 5 ms and that for lysozyme, 50 ms. The pulse sequence used for this experiment is given in Fig. 1A. Appropriate phase cycling was employed for the 2Q and 3Q experiments. The pathway selected in the 2Q MERCY experiment is as follows: $T_{1,0} \xrightarrow{\pi} -T_{1,0} \xrightarrow{\hat{K}} T_{2,0} \xrightarrow{\pi/2} T_{2,\pm 2} \xrightarrow{\pi/2} T_{2,-1}$

longitudinal relaxation [22]. Two-dimensional 2Q and 3Q experiments on the two proteins shown in Fig. 5 isolate the transverse relaxation behaviour. Here we focus on the peaks occurring on the multiple quan-

tum diagonals. These diagonal peaks basically are the signatures of the two- or three-spin orders created in the methyl groups in the protein arising from rank two or three terms. The presence of a large CSR \times DD cross-correlation in HRP-CN causes predominance of two-spin order leading to strong methyl 2Q diagonal peaks in the 2Q spectrum. In contrast the three-spin order characteristic of DD \times DD cross-correlations gives rise to weaker 3Q diagonal peaks in the 3Q spectrum of HRP-CN. In lysozyme,

on the other hand, one observes a prevailing 3Q signature coming from rank 3 terms and a weaker, yet easily observable 2Q signature. The opposite intensity ratio between the 3Q and 2Q experiments for diamagnetic and paramagnetic proteins is the clearest indication of the change in predominance of third and second rank terms generated through cross-correlated relaxation. Simulations shown in Fig. 3 are in accordance with the experiments where the maximum excitation level is achieved at a τ interval of ca. 5 ms of single quantum evolution time for HRP-CN. In the simulations no effect of random field and leakage terms has been taken into account. It must also be realized that there is at least a factor of 4 attenuation of 3QC compared to 2QC by the MQ filter. For these reasons the 3Q peaks appear weaker than the 2Q peaks in Fig. 5C,D though $f_{31}^{(1)}(t)$ is bigger than $f_{21}^{(1)}(t)$ in Fig. 3D. A quantification of the influence of random-field terms will be presented elsewhere.



5. Conclusions

To the best of our knowledge this investigation is the first of its kind dealing with the influence of the cross-correlation terms involving the electron paramagnetic centre on the relaxation patterns of methyl groups in a protein. Both longitudinal and transverse methyl proton relaxation show distinct spectral signatures stemming from the respective dominating relaxation allowed coherence transfer pathways. Two types of multi-quantum experiments exhibit charac-

Fig. 5. The spectra resulting from two-dimensional 2Q and 3Q experiments on lysozyme (A,B) and HRP (C,D) respectively. The pulse sequence used is given in Fig. 1B with appropriate phase cycling to select 2Q or 3Q coherence. The relaxation delay, τ , for HRP was 2 ms and that for lysozyme, 30 ms. For HRP 256 t_1 increments were acquired with an increment of 22 μ s with 96 transients per increment and a relaxation delay of 1 s. For lysozyme 256 t_1 increments were acquired with an increment of 22 μ s with 96 transients per increment and a recycle delay of 1.5 s. A TPPI [35] scheme was employed to achieve quadrature detection in the indirect dimension. The arrow in (D) points to the 2Q diagonal peak characterizing the two-spin order generated in the I-244 γ CH₃ protons, in HRP, predominantly via CSR \times DD cross-correlation. The pathway selected in the 2Q experiment is as follows: $T_{1,0} \xrightarrow{\pi} T_{1,\pm 1} \xrightarrow{\hat{R}} T_{2,\pm 1} \xrightarrow{\pi/2} T_{2,\pm 2} \xrightarrow{\pi/2} T_{2,-1}$.

teristic features due to the presence of cross-correlation terms in methyl groups in absence and presence of an unpaired electron spin. In the 1D 2Q MERCY and the 2D 2Q correlation experiments the creation of two-spin order within the CH₃ group is due to cross-correlation involving CSR and DD terms. In HRP-CN this is shown to be of a greater magnitude than in diamagnetic systems where only the weaker CSA × DD cross-correlation term can give rise to such signals. Numerical simulations of transfer functions are in good accordance with the experimental spectra. Due to the distance and angular dependence of the CSR × DD cross-correlation terms (Eq. (5)) and their considerable magnitude their quantitation should allow to derive additional structural constraints. Since transverse relaxation experiments can independently give distance estimates this can improve structure refinement of paramagnetic proteins in solution. Work is in progress to quantify the influence of CSR × DD cross-correlation terms on molecules which are in other motional regimes.

Acknowledgements

This work was supported by the Austrian Science Foundation (FWF) through project P12696 CHE and a Lise Meitner fellowship for P.K. Madhu (M531-CHE). N.M. also acknowledges a grant from the 'Jubiläumsfonds' of the Austrian National Bank (No. 6808).

References

- [1] H. Shimizu, *J. Chem. Phys.* 40 (1964) 3357.
- [2] S. Wimperis, G. Bodenhausen, *Chem. Phys. Lett.* 140 (1987) 41.
- [3] N. Müller, G. Bodenhausen, R.R. Ernst, *J. Magn. Reson.* 75 (1987) 297.
- [4] J. Keeler, F.S. Ferrando, *J. Magn. Reson.* 75 (1987) 96.
- [5] V.V. Krishnan, Anil Kumar, *J. Magn. Reson.* 92 (1991) 292.
- [6] T.C. Farrar, R.Q. Quintero-Arcaya, *Chem. Phys. Lett.* 122 (1982) 41.
- [7] L.G. Werbelow, in: R. Tycho (Ed.), *Nuclear Magnetic Resonance Probes of Molecular Dynamics*, vol. 223, Kluwer Academic Publ., 1994.
- [8] L.G. Werbelow, D.M. Grant, *Adv. Magn. Reson.* 29 (1978) 189.
- [9] R. Brüschweiler, C. Griesinger, R.R. Ernst, *J. Am. Chem. Soc.* 111 (1984) 8034.
- [10] R. Brüschweiler, R.R. Ernst, *J. Chem. Phys.* 96 (1992) 1758.
- [11] B. Reif, M. Hennig, C. Griesinger, *Science* 276 (1997) 1230.
- [12] R. Wimmer, N. Müller, *J. Magn. Reson.* 129 (1997) 1.
- [13] I. Bertini, C. Luchinat, D. Tarchi, *Chem. Phys. Lett.* 203 (1993) 445.
- [14] J. Qin, F. Delaglio, G.N. La Mar, A. Bax, *J. Magn. Reson.* 102 (1993) 332.
- [15] I. Bertini, C. Luchinat, M. Piccioli, D. Tarchi, *Conc. Magn. Reson.* 6 (1994) 303.
- [16] L. Mäler, F.A.A. Mulder, J. Kowalewski, *J. Magn. Reson. A* 117 (1995) 220.
- [17] R. Ghose, J.H. Prestegard, *J. Magn. Reson.* 128 (1997) 138.
- [18] H. Desvaux, M. Gochin, *Mol. Phys.* 96 (1999) 1317.
- [19] J. Boisbouvier, P. Gans, M. Blackledge, B. Brutscher, D. Marion, *J. Am. Chem. Soc.* 111 (1999) 7700.
- [20] I. Solomon, *Phys. Rev.* 99 (1955) 559.
- [21] N. Bloembergen, *J. Chem. Phys.* 27 (1956) 572.
- [22] M. Gueron, *J. Magn. Reson.* 19 (1975) 58.
- [23] A.J. Vega, D. Fiat, *Mol. Phys.* 31 (1976) 347.
- [24] N. Müller, *Chem. Phys. Lett.* 31 (1986) 218.
- [25] L.G. Werbelow, D.M. Grant, *J. Magn. Reson.* 20 (1975) 554.
- [26] N. Müller, G. Bodenhausen, *J. Chem. Phys.* 98 (1993) 6062.
- [27] G.N. La Mar, G.R. Van Hecke, *J. Chem. Phys.* 52 (1970) 5676.
- [28] A.G. Redfield, *Adv. Magn. Reson.* 1 (1965) 1.
- [29] D.M. Brink, G.R. Satchler, *Angular Momentum*, Oxford University Press, London, 1968.
- [30] J. de Ropp, P.K. Mandal, G.N. La Mar, *Biochemistry* 38 (1999) 1077.
- [31] M. Gajhed, D.J. Schuller, A. Henriksen, A.T. Smith, T.L. Poulous, *Nature Struct. Biol.* 4 (1997) 1032.
- [32] J. de Ropp, G.N. La Mar, *J. Am. Chem. Soc.* 110 (1996) 3027.
- [33] I. Bertini, C. Luchinat, *Coordination Chem. Rev.* 150 (1996) 77.
- [34] W. Kutzelnigg, U. Fleischer, M. Schindler, *NMR Basic Principles and Progress*, Springer, Berlin 23, 1990, pp. 165.
- [35] G. Drobny, A. Pines, S. Sinton, D. Weitekamp, D. Wemmer, *Faraday Div. Chem. Soc. Symp.* 13 (1979) 49.